

# A Compact High-Performance Orthomode Transducer for the Atacama Large Millimeter Array (ALMA) Band 1 (31–45 GHz)

DAVID DOUSSET<sup>1</sup>, STÉPHANE CLAUDE<sup>2</sup>, AND KE WU (Fellow, IEEE)<sup>1</sup>

<sup>1</sup>Poly-Grames Research Center, Département de Génie Électrique, École Polytechnique de Montréal, Montréal, QC H3T1J4, Canada

<sup>2</sup>National Research Council - Herzberg, Victoria, BC V9E 2E7, Canada

Corresponding author: D. Dousset (david.dousset@polymtl.ca)

**ABSTRACT** This paper describes a compact high-performance orthomode transducer (OMT) with a circular waveguide input and two rectangular waveguide outputs based on the superimposition of three aluminum blocks. Several prototypes operating in the band 1 (31–45 GHz) of the atacama large millimeter array have been fabricated and measured. The design is based on the use of a turnstile junction that is machined in a single block, requiring neither alignment nor a high degree of mechanical tolerances. Thus, a high repeatability of the design is possible for mass production. Across the 31–45 GHz band, the isolation is better than 50 dB and the return losses at the input and outputs of the OMT are better than –25 dB.

**INDEX TERMS** Radio astronomy, orthomode transducer (OMT), turnstile junction, polarization diplexer.

## I. INTRODUCTION

An orthomode transducer (OMT), which allows to combine or separate two orthogonal polarizations within the same frequency band, represents a very interesting alternative to a conventional quasi-optical wire grid polarizer for cryogenic low noise receivers in the domain of radio astronomy and for communication systems [1]. Indeed, when an OMT is used, only one feed horn is required, thus reducing the dimensions of the cryostat and the alignment problems with the incoming signal. An OMT is required for a wideband dual-polarization over the 31–45 GHz (Band 1) radio astronomy band of the Atacama Large Millimeter Array (ALMA). Given the number of ALMA antennas and spare, 73 Band 1 OMTs would be required. This band will provide high-resolution images of the evolution of grains in disks around stars and detect molecular gas in the first generation of galaxies [2]. An OMT generally consists of a three-port network, an input port with square or circular waveguide cross section (to interface with the feed horn) and two full-height rectangular waveguide output ports, one output for each polarization. The specifications for the ALMA Band 1 OMT are the following; isolation levels higher than 40 dB and return losses lower than –18 dB. The OMT must be made as compact as possible to fit into the limited prescribed volume and easy to manufacture since 73 units have to be delivered to ALMA. Several types of OMTs were

proposed in the literature. Some of them are based on a Bøifot junction, by using a septum with matching pins or capacitive steps in waveguide walls to improve the return losses, and also to discriminate two orthogonal polarizations [3] and [4]. Other OMT designs may consist of a square to double or quad-ridged waveguides to split the incoming polarizations [5] and [6]. Alignments of separate pieces and the machining of very small matching pins or ridged waveguides can be delicate, particularly for OMTs operating above 100 GHz. This design could therefore prove to be difficult to be reliably produced in a large volume. More recently, a number of authors proposed OMTs based on the use of waveguide backward coupling structures that act as polarization splitters [7]–[9]. The main advantage here is that neither septum nor pins are required to achieve polarization separation. The most interesting OMTs in terms of isolation performance over a large bandwidth are turnstile junction based OMTs [10]–[12]. A turnstile junction consists of a circular or square waveguide input port and four rectangular waveguide outputs. Navarrini et al. [10] showed that very good isolation level and return-loss coefficients could be obtained across the K-band. However, the main drawback of the proposed design is that the OMT is based on the use of a turnstile junction from four blocks that intersect along the circular waveguide (CWG) axis. This particularity makes the scaling of this OMT

design difficult at higher frequencies due to alignment issues. In this paper, we present an alternative approach to the OMT proposed by Navarrini et al. Indeed, our mechanical design, which consists of three superimposed blocks, allows us to machine the waveguide cylinder input and the matching stub in only one step using a computer numerically controlled (CNC) milling machine. Outside dimensions and measurements of our design was presented in [13] and [14] within the context of the ALMA Band 1 cartridge design. We describe details of the structure as well as measurements of this OMT operating in the ALMA Band 1. Also, in order to verify the repeatability of the proposed design in anticipation of a production run, measurement results of four prototypes are presented.

## II. THEORY AND DESIGN OF THE OMT

Our new OMT is based on the use of a turnstile junction in order to separate two orthogonal polarizations within the same frequency band. Indeed, the turnstile junction is a key element for OMT designs for high performance in terms of polarization isolation and return loss. It consists of a circular waveguide at the input and four rectangular waveguide outputs, as shown in Fig. 1. Each of the two incoming polarizations, Pol. 1 and Pol. 2, at the circular waveguide input and coming from the horn antenna, is equally separated by the turnstile junction in two  $180^\circ$  out-of-phase RF signals, called Pol. 1+, Pol. 1- and Pol. 2+, Pol. 2-, respectively. Thus, the two polarizations can be simultaneously processed without the need to use a wire-grid diplexer and two horns antennas.

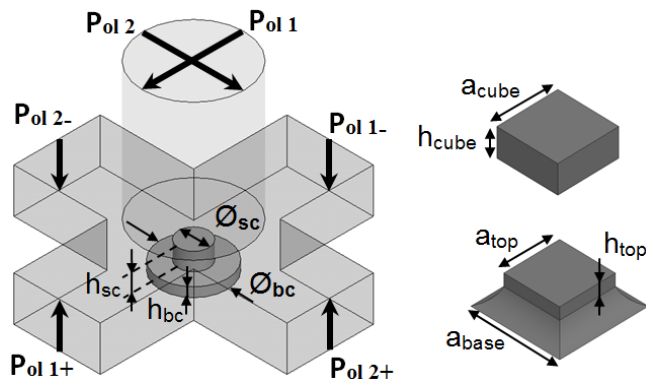


**FIGURE 1.** Turnstile junctions with three possible matching stubs (a parallelepiped, a truncated pyramid and two superimposed cylinders).

ALMA Band 1 covers 31–45 GHz and this is dictated by key astronomical molecular lines that need to be observed. The closest standard communication band is the Q band that covers 33–50 GHz. In order to optimize the OMT all the way down to 31 GHz, the dimensions of the output rectangular waveguides were modified to  $6.33 \times 3.25$  mm (called band 1 waveguide to simplify writing). Also, the input circular waveguide radius, matched to a feedhorn in the Band 1 system is 3.71 mm.

For high performance OMTs, with high polarization isolation, the return loss at the circular waveguide input must be carefully optimized using a matching element placed at the center of the turnstile junction. Various matching structures were investigated and simulated to identify the best return loss ( $S_{11}$ ) over the largest bandwidth (see Fig. 1). Given the fact that the turnstile is made of two waveguides crossing, a simple and natural matching stub is a parallelepiped to fill in part of the central cavity. After optimization of the height and width of the parallelepiped ( $a_{cube} = 2.97$  mm and  $h_{cube} = 1.27$  mm), using HFSS [15] with aluminum conductivity of  $3.8 \times 10^7$  S/m, the return loss was found to be below  $-25$  dB for the Band 1 operating band (see Fig. 2), i.e. 31–45 GHz. Matching can be further improved by providing a more gradual change in the direction of the input circular waveguide. Therefore, a pyramid would be well suited but not simple to machine while preserving symmetry and a sharp end. Rather, a truncated pyramid [10] as described in Fig. 1 is easier to machine. The truncated pyramid has the following dimensions:  $a_{base} = 4.56$  mm;  $\phi_{fillet} = 1$  mm,  $h_{base} = 0.84$  mm,  $a_{top} = 2.67$  mm and  $h_{top} = 0.6$  mm. A few dB of improvements were obtained compared to the parallelepiped. The pyramid can also be simplified into a stack of disks [11] as shown in Fig. 1. Diameters and heights of the superimposed cylinders are the following;  $\phi_{bc} = 4.9$  mm,  $\phi_{sc} = 2.2$  mm,  $h_{bc} = 0.68$  mm and  $h_{sc} = 1.29$  mm, respectively. Simulated return losses as shown in Fig. 2 show dramatic improvements in midband with  $S_{11}$  of  $-40$  dB instead of  $-25$  dB obtained using the parallelepiped.

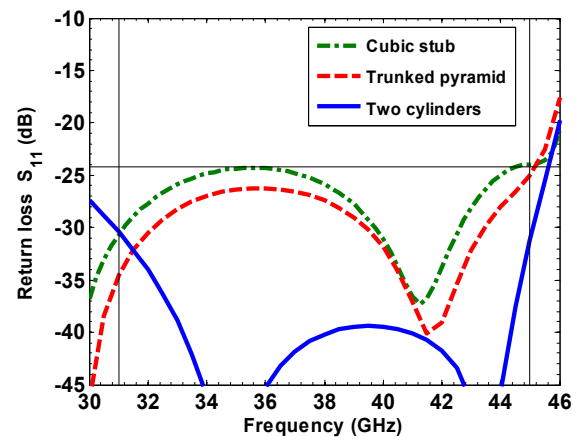
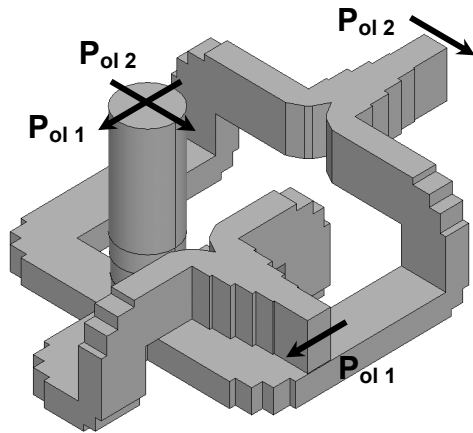


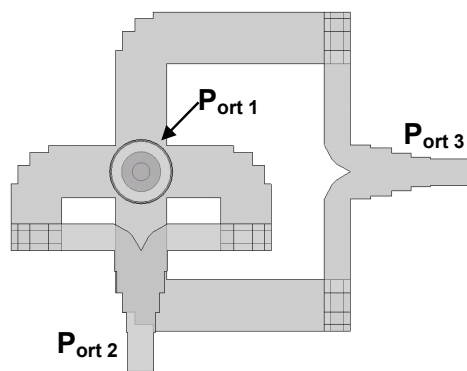
**FIGURE 2.** Simulated return losses  $S_{11}$  at the circular waveguide input of the turnstile junction for three different matching elements.

Very good positioning of the matching element, in the center of the turnstile junction, is crucial in order to efficiently separate the two orthogonal polarizations. Otherwise, RF performances could be significantly deteriorated. The concept of our OMT design is based on the following rules: 1) the matching element should not be split into four identical blocks intersecting on the axis of the input circular waveguide (as described in [16]); 2) the matching element should not be a mobile part to be glued, screwed, soldered or just

inserted in the center of the turnstile junction (as described in [16] and [17]); and 3) the total number of blocks to assemble the OMT should be minimized. Respecting these rules is possible with the final structure of the OMT presented in Fig. 3(a) and 3(b).



(a)



(b)

**FIGURE 3. (a) Polarizations at the input and the two outputs of the OMT. (b) Designation of the input and outputs ports of the OMT (top view).**

For each polarization, an E-plane  $180^\circ$  out-of-phase power combiner is used in order to recombine the RF signals split by the turnstile junction through opposite waveguide outputs.

From a practical point of view, the final structure of the OMT presented in Fig. 3(a) and 3(b) is realized by superimposing three aluminum blocks (see Fig. 4).

The upper block consists of a circular waveguide input, a circular waveguide transition, two E-plane power combiners and four H-plane  $90^\circ$  bends (as shown in Fig. 5(a)). The lower block consists of the base of the turnstile junction with two superimposed cylinders as a matching stub, four H-plane  $90^\circ$  bends and four E-plane  $90^\circ$  bends (as depicted in Fig. 5(b)). The middle aluminum block acts as an interface between the lower and upper blocks, connecting the outputs of the turnstile junction to the inputs of the power combiners. Also, it directs the signal coming from the circular waveguide input towards the base of the turnstile junction. The novelty of this OMT

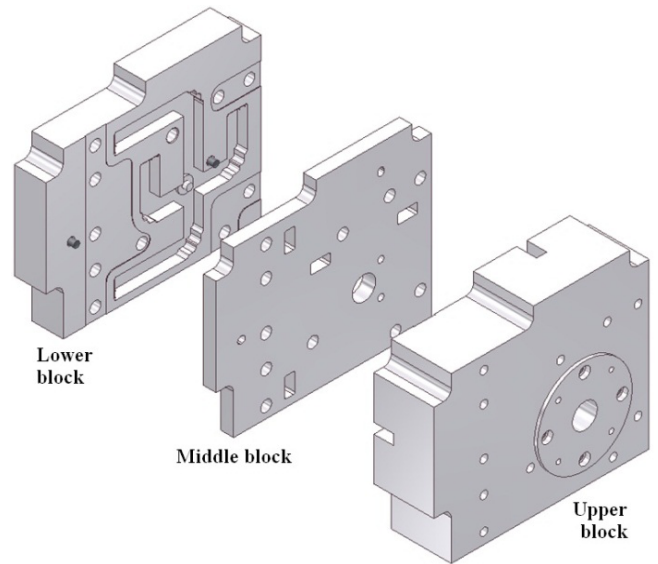
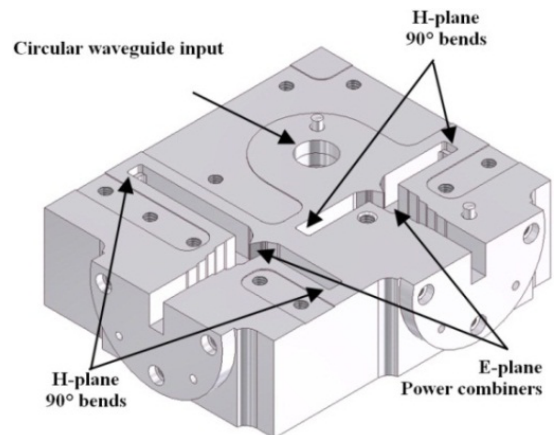
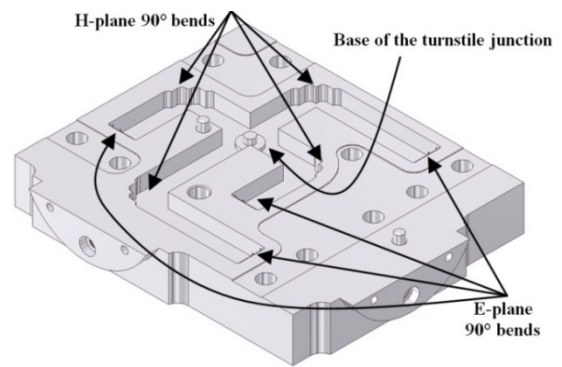


**FIGURE 4. Exploded view of the mechanical design of the OMT.**



(a)



(b)

**FIGURE 5. (a) Upper aluminum block of the OMT. (b) Lower aluminum block of the OMT.**

is that the core of the turnstile junction, i.e. the matching element and the four rectangular waveguide outputs is machined in one single block, therefore optimizing the accuracy of this

key element. This allows scaling to shorter wavelengths for OMTs operating at a few hundred GHz, within the standard limits of the CNC accuracy.

Furthermore, the use of compact 90° bends and power combiners as described below, allow the two waveguide ports to be located on any face, i.e. 90° to the input, or in line with the input on the opposite side or, if required, on the same face as the input port. Because the matching element located at the center of the turnstile junction is not higher than the height of the band 1 rectangular waveguide, it is much easier to machine the lower aluminum block. Thus, mass production can be considered at low cost and low manufacturing time.

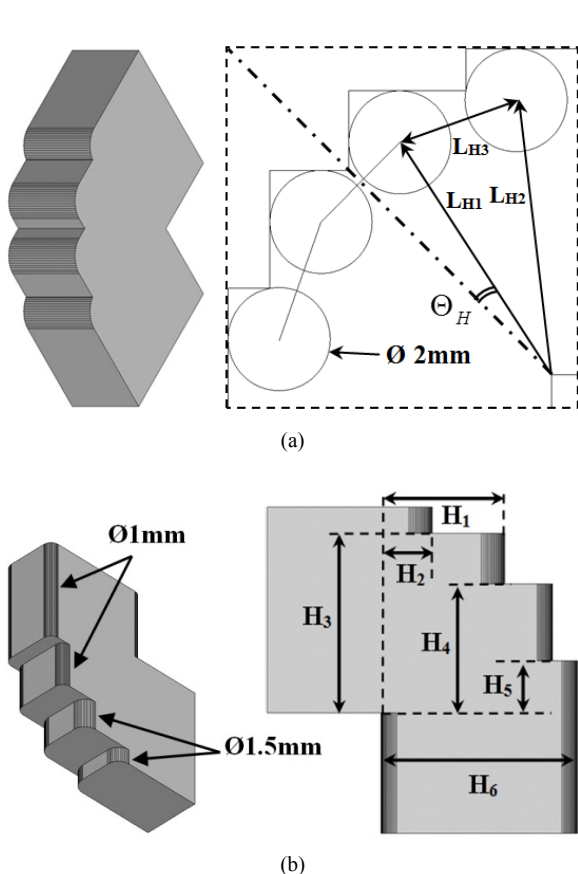


**FIGURE 6.** (a) 3-step H-plane bend when milling is done parallel to the narrow walls of the waveguide. (b) 3-step H-plane bend when milling is done perpendicular to the narrow walls of the waveguide.

In order to limit the number of assembling blocks to three and to make the OMT as compact as possible, bends with a right angle are preferred [18], [19]. The design includes round corners that result from milling with a conventional CNC machine. Fig. 6(a) and 6(b) depicts two 3-step H-plane bends. In the first case, milling is performed parallel to the narrow walls of the waveguide. Physical dimensions with a 2 mm diameter end mill are;  $\Theta_H = 11.7^\circ$ ,  $L_{H1} = 5.4$  mm,  $L_{H2} = 5.37$  mm and  $L_{H3} = 2.43$  mm. For the second bend (with perpendicular milling), two different standard diameters of end mills were used because larger end mills can cut deeper

(see Fig. 6(b)). For shallow cuts a 1 mm diameter end mill was used. For deeper cuts, corresponding to the total width of the broad walls of the waveguide, a 1.5 mm end mill was chosen. Physical dimensions for this bend are the following;  $H_1 = 3.98$  mm,  $H_2 = 1.64$  mm,  $H_3 = 5.52$  mm,  $H_4 = 3.96$   $\mu$ m,  $H_5 = 1.6$  mm and  $H_6 = 6.33$  mm.

Fig. 7(a) shows a 3-step E-plane bend when the milling is performed parallel to the narrow walls of the waveguide. Physical dimensions for this bend (using a standard 1 mm diameter end mill) are the following;  $E_1 = 2.5$  mm,  $E_2 = 2$  mm,  $E_3 = 0.67$  mm,  $E_4 = 2.01$  mm,  $E_5 = 0.66$  mm,  $E_6 = 2.5$  mm and  $E_7 = 3.25$  mm.

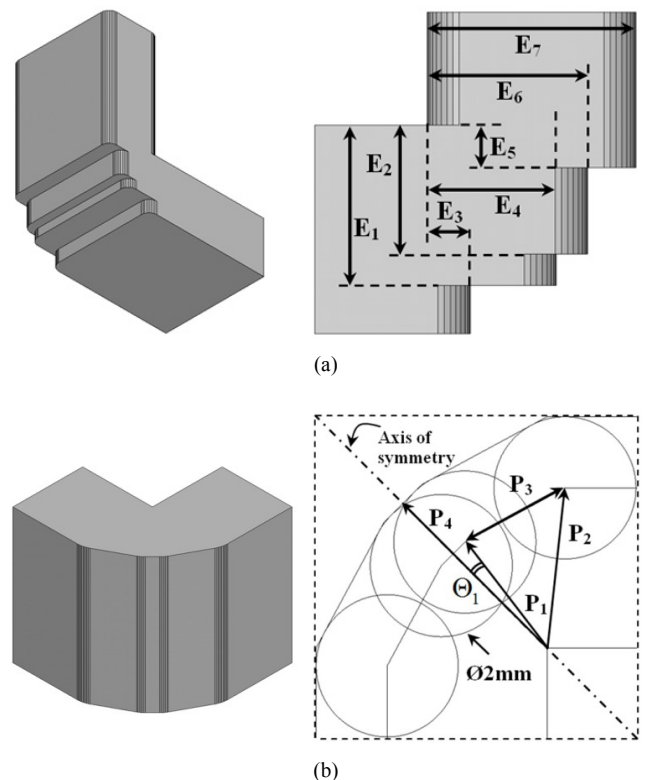


**FIGURE 7.** (a) 3-step E-plane bend when the milling is done parallel to the narrow walls of the waveguide. (b) 3-miter E-plane bend when the milling is done perpendicular to the narrow walls of the waveguide.

Fig. 7(b) presents a 3-miter E-plane bend. In this last case the milling is done perpendicular to the narrow wall of the waveguide. Physical dimensions are the following (using a standard 2 mm diameter end mill);  $P_1 = 1.88$  mm,  $P_2 = 2.26$  mm,  $P_3 = 1.6$  mm,  $P_4 = 2.87$  mm and  $\Theta_1 = 15.1^\circ$ .

Simulated return losses as a function of frequency for the four bends are shown in Fig. 8. In all cases, the reflection coefficient is maintained below  $-44$  dB over the 31–45 GHz band. These excellent results of compact devices can all be reached using standard end-mill diameters.

In order to recombine signals which are split by the turnstile junction, an E-plane power combiner in a Y-junction configuration was designed. This type of bend, consisting of a multi-step impedance transformer and two E-plane bends

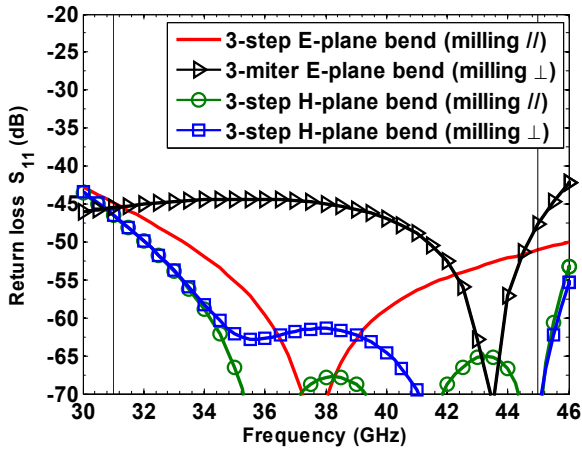


FIGURE 8. Simulated return losses,  $S_{11}$ , for the two H-plane bends and the two E-plane bends.

placed at the wide section of the transformer (forming a Y-junction), was previously proposed by A. R. Kerr [20]. For a more efficient and compact power combiner, we make use of a 4-section transformer and two 3-miter E-plane bends. As we can see in Fig. 9, the return loss at the input of the power combiner is below  $-40$  dB over our band of interest. In order to keep a finite thickness during the manufacturing process, a cusp at the intersection (Fig. 9) of the two-miter bends is truncated at a width of  $0.1$  mm. In order to be able to machine the 4-section transformer and the 3-miter bends on a cut length of  $6.33$  mm (represents the full width of the band 1 waveguide), a standard  $2$  mm-diameter end-mill was used.

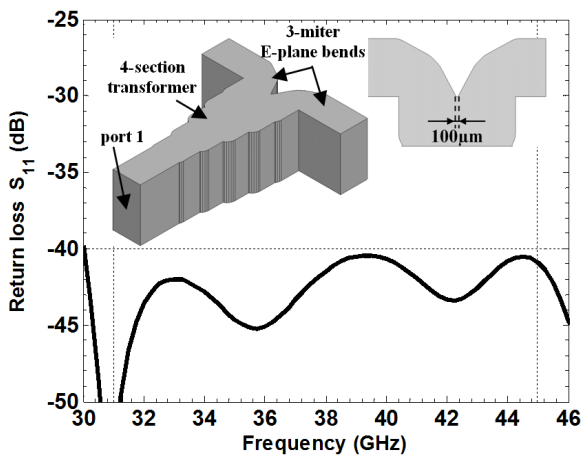
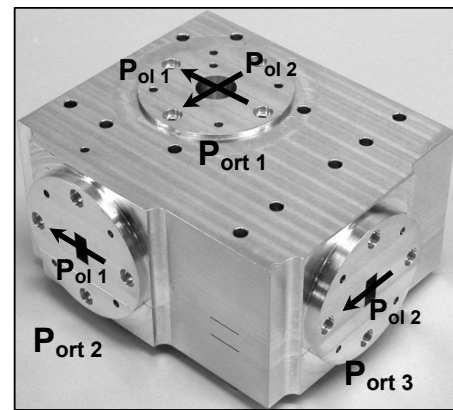


FIGURE 9. Structure and simulated return losses at the input of the compact E-plane power combiner.

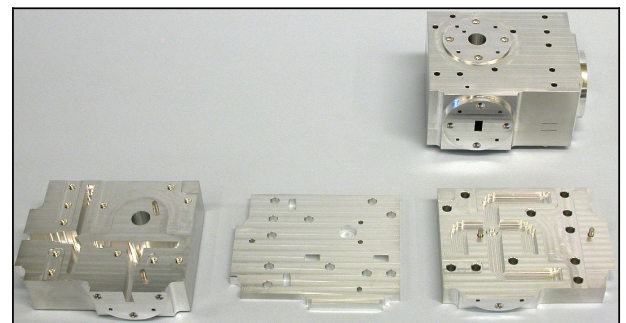
### III. EXPERIMENTAL VERIFICATION OF THE OMT

The structure of the OMT presented in Fig. 4 is realized by superimposing three aluminum blocks made of Aluminum 6061 with a T6 temper (see Fig. 10(a) and 10(b)). The three parts are machined using a CNC milling machine and two dowel pins are used for alignment. The machining required

for the manufacturing of this OMT is standard for a CNC machine with tolerance within reach of a production-type workshop. The dowel pins and the features of the turnstile and bends have  $\pm 0.01$  mm tolerances which is the tightest tolerance in the OMT. The rest of the features have  $\pm 0.02$  mm and  $\pm 0.1$  mm tolerances. The RF design is optimized so that a high level of tolerance is not required in the manufacturing. Therefore, this prototype could be reproduced at a larger scale without compromising performance. In addition, this makes scaling of the design easy to sub-millimeter frequencies. Overall dimensions of the prototype are  $34$  mm  $\times$   $52$  mm  $\times$   $68$  mm.



(a)



(b)

FIGURE 10. (a) Photograph of the assembled OMT with polarizations. (b) Photograph of the OMT before and after the assembly.

In order to evaluate the reliability of the machining process for production development of our OMT, four prototypes were manufactured and measured. An Anritsu 37397C vector network analyzer (VNA) was used to measure S-parameters of the OMTs in the  $30$ – $46$  GHz frequency band. The configuration for the isolation (between ports 2 and 3) and return loss measurements at the rectangular waveguide outputs (at ports 2 and 3) is shown in Fig. 11. A short, short load and thru (SSLT) calibration was performed to eliminate systematic uncertainties and to shift the reference planes to the WR-22 flange of the coaxial-waveguide transition.

Simulated and measured results for all the prototypes show an isolation level between the two rectangular waveguide

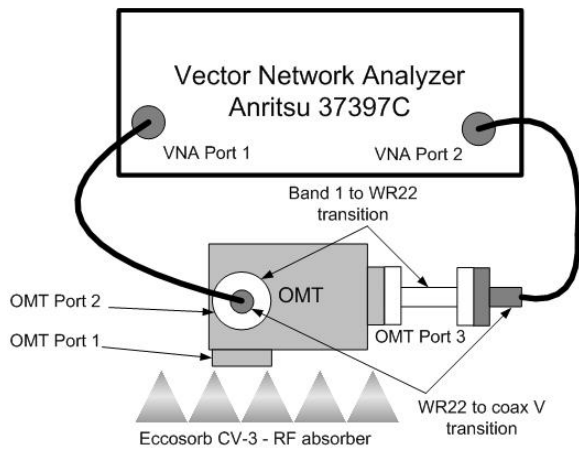


**FIGURE 11.** Configuration used to measure the isolation levels ( $S_{32}$ ) and return losses ( $S_{22}$  and  $S_{33}$ ).

outputs better than 50 dB (as shown in Fig. 12). The discrepancies observed across the band between the measured isolations are due to the difficulty - at the time of the measurements - of placing the absorbing material in the same way at the CWG inputs of the OMTs.

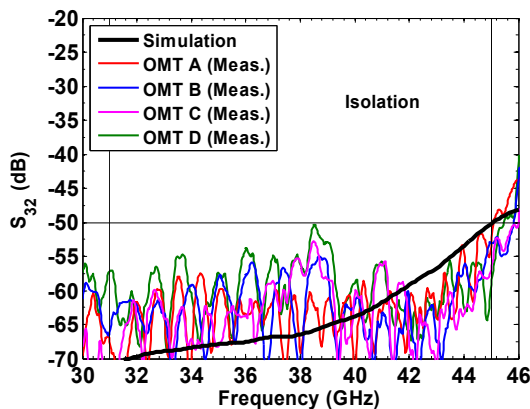


**FIGURE 12.** Measured isolation level ( $S_{32}$ ) between the two rectangular waveguide outputs of the four OMT prototypes.

Simulated and measured return losses at the RWG outputs of the OMTs, called ports 2 and 3, are presented in Fig. 13(a) and 13(b). In all cases, the measured return losses,  $S_{22}$  and  $S_{33}$ , at the two rectangular waveguide (RWG) outputs are excellent because they are below  $-25$  dB in the band of interest.

Discrepancies are observed between the simulated and measured return losses. The fact that measured return loss levels are below  $-25$  dB means less than 0.3% of the incident power is reflected. This small amount of lost power is easily attributed to a non-perfect flange mating between the rectangular outputs of the OMTs and the transitions from Band 1 to WR-22 waveguides connected at ports 2 and 3. Machining quality of the corners of the Band 1 to WR-22 transitions might also have contributed to the slight degradation of the return losses.

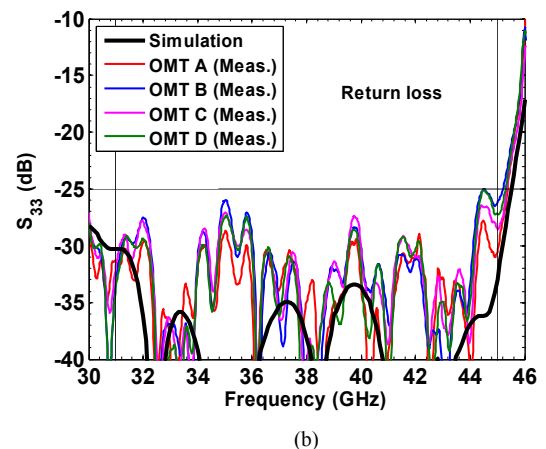
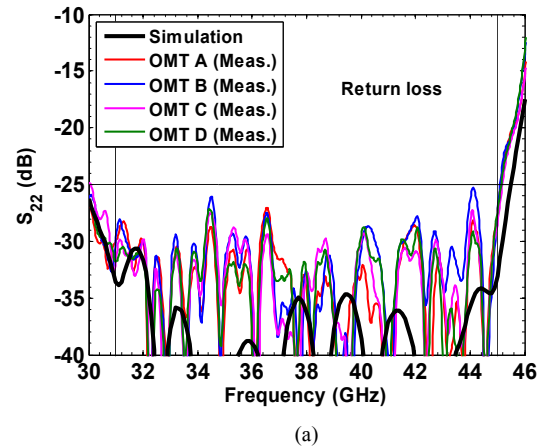


**FIGURE 13.** (a) Simulated and measured return losses of port 2 of the four OMTs. (b) Simulated and measured return losses of port 3 of the four OMTs.

#### IV. CONCLUSION

In this paper, an orthomode transducer (OMT) with a circular waveguide input and two rectangular waveguide outputs for the ALMA Band 1 (31–45 GHz) was studied, designed, manufactured and measured. The OMT consists of a matched turnstile junction that uses two superimposed cylinders placed at the base of the junction, and two wide-band power combiners. Assembly of the OMT is realized by superimposing three aluminum blocks. In this way, the integrity of both the circular waveguide input and the matching stub are maintained. Thus, there is no need to reconstruct them from blocks that intersect along the circular axis, which eliminates alignment problems between block halves. Furthermore, they can be machined in only one step using a CNC milling machine with standard machining tolerances without the necessity of using high aspect ratio tool bits. The proposed design is suitable for scaling to sub-millimeter wavelengths. All four OMT prototypes show very good and almost identical performance. The return losses at the inputs and outputs of the four OMT prototypes are better than  $-25$  dB. Average insertion losses, at room temperature, are lower than 0.2 dB. Both polarizations and isolation levels between the two rectangular waveguide outputs are higher than 50 dB in the 30.5–45.5 GHz

(37% bandwidth). Those excellent results meet the stringent requirements of ALMA Band 1. Furthermore, a very good reproducibility can be obtained during the manufacturing and assembling phases of the OMTs, demonstrating that mass production is feasible.

## REFERENCES

- [1] J. Uher, J. Bornemann, and U. Rosenberg, *Waveguide Components for Antenna Feed Systems: Theory and CAD*. Norwood, MA, USA: Artech House, 1993.
- [2] D. Johnstone, J. Di Francesco, B. Matthews, N. Bartel, L. Bronfman, S. Casassus, S. Chitsazzadeh, M. Cunningham, G. Duchene, A. Hales, M. Houde, D. Iono, P. M. Koch, R. Kothes, S.-P. Lai, S.-Y. Liu, B. Mason, T. Maccarone, G. Schieven, A. M. M. Scaife, D. Scott, H. Shang, S. Takakuwa, J. Wagg, A. Wootten, and F. Yusef-Zadeh. (2010). *The Science Case for Building a Band 1 Receiver for ALMA* [Online]. Available: [http://arxiv.org/PS\\_cache/arxiv/pdf/0910/0910.1609v2.pdf](http://arxiv.org/PS_cache/arxiv/pdf/0910/0910.1609v2.pdf)
- [3] G. Narayanan and N. Erickson, "Full-waveguide band orthomode transducer for the 3 mm and 1 mm bands," in *Proc. 14th Int. Symp. Space Terahertz Technol.*, Apr. 2003, pp. 508–512.
- [4] J. A. Ruiz-Cruz, J. R. Montejó-Garai, J. M. Rebolgar, C. E. Montesano, and M. J. Martín, "Very compact ortho-mode transducers with double septum configuration," *Microw. Opt. Technol. Lett.*, vol. 48, no. 4, pp. 765–767, Apr. 2006.
- [5] S. Asayama and M. Kamikura, "Development of double-ridged waveguide orthomode transducer for the 2 MM band," *J. Infr., Millim. Terahertz Waves*, vol. 30, no. 6, pp. 573–579, Jun. 2009.
- [6] Z. Zhuang, B. Li, and Q. Fan, "Design of improved quad-ridged orthomode transducer," in *Proc. ICMMT*, May 2010, pp. 867–70.
- [7] A. Navarrini and R. Nesti, "Symmetric reverse-coupling waveguide orthomode transducer for the 3-mm band," *IEEE Trans. Microw. Theory Tech.*, vol. 57, no. 1, pp. 80–88, Jan. 2009.
- [8] O. A. Peverini, R. Tascone, G. Virone, A. Olivieri, and R. Orta, "Orthomode transducer for Millim.-wave correlation receivers," *IEEE Trans. Microw. Theory Tech.*, vol. 54, no. 5, pp. 2042–2048, May 2006.
- [9] C. Groppi, A. Navarrini, and G. Chattopadhyay, "A waveguide orthomode transducer for 385–500 GHz," in *Millimeter, Submillimeter, and Far-Infrared Detectors and Instrumentation for Astronomy V*, vol. 7741, W. S. Holland and J. Zmuidzinas, Eds. Bellingham, WA, USA: SPIE, 2010, pp. 7741–7786.
- [10] A. Navarrini and R. L. Plambeck, "A turnstile junction waveguide orthomode transducer," *IEEE Trans. Microw. Theory Tech.*, vol. 54, no. 1, pp. 272–277, Jan. 2006.
- [11] M. A. Meyer and H. B. Golberg, "Applications of the turnstile junction," *IRE Trans. Microw. Theory Tech.*, vol. 3, no. 6, pp. 40–45, Dec. 1955.
- [12] Y. Aramaki, N. Yoneda, M. Miyazaki, and T. Horie, "Ultra-thin broadband OMT with turnstile junction," in *IEEE MTT-S Int. Microw. Symp. Dig.*, vol. 1, Jun. 2003, pp. 47–50.
- [13] S. Claude, F. Jiang, D. Dousset, N. Wren, I. Wevers, M. Fletcher, D. Henke, and K. Wu, "ALMA band 1 (31–45 GHz) receiver development at HIA," in *Proc. Conf. AAS Meeting*, Jun. 2009, p. 568.
- [14] D. Henke, S. Claude, and F. Jiang, "Component development for ALMA Band 1 (31–45 GHz)," in *Millimeter, Submillimeter, and Far-Infrared Detectors and Instrumentation for Astronomy V*, vol. 7741, W. S. Holland and J. Zmuidzinas, Eds. Bellingham, WA, USA: SPIE, 2010, pp. 7741–7775.
- [15] *High Frequency Structure Simulator (HFSS), Version 11*, Ansoft Corp., Pittsburg, PA, USA, 1995.
- [16] A. Navarrini, A. Bolatto, and R. L. Plambeck, "Test of 1 mm band turnstile junction waveguide orthomode transducer," in *Proc. 17th Int. Symp. SIT*, 2006, pp. 99–102.
- [17] A. Tribak, A. M. Sanchez, A. C. Lopez, and K. Cepero, "A dual linear polarization feed antenna system for satellite communications," *PIERS Online*, vol. 7, no. 3, pp. 236–240, 2011.
- [18] N. Marcuvitz, *Waveguide Handbook, by Peregrinus on Behalf of The Institution of Electrical Engineers*. New York, NY, USA: Dover, 1986.
- [19] M. Zhewang, T. Yamane, and E. Yamashita, "Analysis and design of H-plane waveguide bends with compact size, wide-band and low return loss characteristics," in *IEEE MTT-S Int. Microw. Symp. Dig.*, vol. 2, 1997, pp. 417–420.
- [20] A. R. Kerr, "Elements for E-plane split-blocks waveguide circuits," NRAO, Charlottesville, VA, USA, ALMA Memo 381, Jul. 2001.



**DAVID DOUSSET** received the B.Sc. degree in electrical engineering from Polytech Nantes, Nantes, France, in 2000, and the M.Sc.A. and Ph.D. degrees from École Polytechnique de Montréal, Montréal, QC, Canada, in 2003 and 2010, respectively. In 2003, he was a Research Associate with the Electrical Engineering Department, École Polytechnique de Montréal, where he developed BJT and HBT transistors models for power amplifier applications. In 2010, he joined the Poly-

Grames Research Center, Montréal, which is affiliated with the École Polytechnique de Montréal. His current research interests include transistor modeling and designs of antennas, passive and active components in the millimeter wave frequency range combined with the low-loss substrate integrated circuit technology. He is currently coordinator of the Center for Radiofrequency Electronics Research of Quebec (Regroupement stratégique de FRQNT).



**STÉPHANE CLAUDE** received the Engineering degree in material sciences from École Nationale Supérieure d'Ingénieurs de Caen, Caen, France, in 1990, and the Ph.D. degree in physics from London University, Queen Mary, and Westfield College, London, U.K., in 1996. From 1990 to 1996, he was a Research Associate with the Rutherford Appleton Laboratory, Chilton, U.K., where he developed techniques for the fabrication of superconducting-insulator-superconducting mixer chips, for low noise sub-millimetre receivers in radio-astronomy. His Ph.D. work was to commission a 500 GHz receiver at the James Clerk Maxwell Telescope (JCMT), Hawaii. In 1996, he joined the Herzberg Institute of Astrophysics, Victoria, BC, Canada, where he continued development on low noise receivers for astronomy, including a 200 GHz receiver for the JCMT and a sideband separating mixer design. From 2000 to 2002, he joined the Institut de Radioastronomie Millimétrique, Grenoble, France, on the design of a 275–370 GHz receiver (Band 7) for the atacam large millimetre array (ALMA). Since 2002, he has been leading the Millimetre Instrumentation Team, Herzberg Institute of Astrophysics, Victoria, BC. He was a Project Engineer for the 84–116 GHz receiver (Band 3) developed for the ALMA. He is an Adjunct Professor with the University of Victoria. His current research interests include millimetre wave low noise receivers and phased array feeds for radio astronomy.



**KE WU** (M'76–SM'81–F'87) received the B.Sc. degree (with distinction) in radio engineering from the Nanjing Institute of Technology (now Southeast University), Nanjing, China, in 1982, and the D.E.A. and Ph.D. degrees in optics, optoelectronics, and microwave engineering (with distinction) from Institut National Polytechnique de Grenoble, Grenoble, France, and University of Grenoble, Grenoble, in 1984 and 1987, respectively. He is a Professor of electrical engineering, and Tier-I Canada Research Chair in RF and millimeter-wave engineering with École Polytechnique (University of Montreal), Montreal, QC, Canada. He holds the first Cheung Kong endowed chair professorship (visiting) with Southeast University, the first Sir Yue-Kong Pao chair professorship (visiting) with Ningbo University, Ningbo, Japan, and an honorary professorship with the Nanjing University of Science and Technology, Nanjing, the Nanjing University of Post Telecommunication, Nanjing, and the City University of Hong Kong, Hong Kong. He has been the Director of the Poly-Grames Research Center and the Founding Director of the Center for Radiofrequency Electronics Research of Quebec (Regroupement stratégique of FRQNT). He has held guest and visiting professorship at many universities around the world. He has authored or co-authored over 930 referred papers, and a number of books/book chapters, and filed more than 30 patents. His current research interests include involve substrate integrated circuits, antenna

arrays, advanced CAD and modeling techniques, wireless power transmission and harvesting, and development of low-cost RF and millimeter-wave transceivers and sensors for wireless systems and biomedical applications, and the modeling and design of microwave photonic circuits and systems. He is a member of the Electromagnetics Academy, the Sigma Xi Honorary Society, and the URSI. He has held key positions in and has served on various panels and international committees, including the chair of technical program committees, international steering committees, and international conferences/symposia. He was the General Chair of the 2012 IEEE MTT-S International Microwave Symposium. He has served on the editorial/review boards of many technical journals, transactions, proceedings, and letters as well as scientific encyclopedia, including editors and guest editors. He is currently the Chair of the joint IEEE Chapters of MTT-S/APS/LEOS, Montreal. He is an elected IEEE MTT-S AdCom Member for from 2006 to 2015 and served as a Chair of the IEEE MTT-S Transnational Committee and Member and Geographic Activities Committee among many other AdCom functions. He was a recipient of many awards and prizes, including the first IEEE MTT-S Outstanding Young Engineer Award, the 2004 Fessenden Medal of the IEEE Canada and the 2009 Thomas W. Eadie Medal of the Royal Society of Canada, and the Queen Elizabeth II Diamond Jubilee Medal. He is a fellow of the Canadian Academy of Engineering and the Royal Society of Canada (The Canadian Academy of the Sciences and Humanities). He was an IEEE MTT-S Distinguished Microwave Lecturer from 2009 to 2011.

• • •